FISEVIER

Contents lists available at ScienceDirect

Biochemical and Biophysical Research Communications

journal homepage: www.elsevier.com/locate/ybbrc



The structure of *Deinococcus radiodurans* transcriptional regulator HucR retold with the urate bound



SooHo Rho ^a, WeonSeok Jung ^a, Jeong Kuk Park ^a, Min Hee Choi ^a, MinJu Kim ^a, JooYoung Kim ^a, JiWon Byun ^a, Taehyun Park ^b, Byung Il Lee ^b, Steven P. Wilkinson ^c, SangYoun Park ^{a,*}

- ^a School of Systems Biomedical Science and Integrative Institute of Basic Sciences, Soongsil University, Seoul, Republic of Korea
- ^b Research Institute, National Cancer Center Korea, Goyang, Gyeonggi, Republic of Korea
- ^c Chemistry and Biochemistry Department, California Polytechnic State University, San Luis Obispo, CA, USA

ARTICLE INFO

Article history: Received 21 April 2022 Received in revised form 28 April 2022 Accepted 11 May 2022 Available online 13 May 2022

Keywords:
HucR
MarR
Repressor
Urate
Uric acid
X-ray crystallography

ABSTRACT

HucR is a MarR family protein of *Deinococcus radiodurans*, which binds tightly to the intergenic region of *HucR* and the uricase gene to inhibit their expression. Urate (or uric acid) antagonizes the repressor function of HucR by binding to HucR to impede its association with the cognate DNA. The previously reported crystal structure of HucR was without the bound urate showing significant structural homology to other MarR structures. In this paper, we report the crystal structure of HucR determined with the urate bound. However, despite the fact that the urate is found at a site well-known to harbor ligands in other MarR family proteins, the overall HucR structure indicates that no significant change in structure takes place with the urate bound. Structure analysis further suggests that the urate interaction in HucR is mediated by histidine/glutamate side chains and ordered water molecules stabilized by various residues. Such interaction is quite unique compared to other known structural interactions between urate and its binding proteins. Furthermore, structural comparison of the apo- and the urate bound forms allows us to hypothesize that the Trp20-mediated water network in the apo-form stabilizes the proper HucR fold for cognate DNA binding, and that urate binding, also *via* Trp20, and the consequent reorganization of water molecules in the binding pocket, likely disrupts the DNA binding configuration to result in the attenuated DNA binding.

© 2022 Elsevier Inc. All rights reserved.

1. Introduction

The extremophilic bacterium *Deinococcus radiodurans* not only withstands ionizing radiations but also has high resistance to various stresses including toxins, antibiotics and oxidation along with multiple others [1,2]. The MarR (Multiple antibiotic resistance Regulator) family proteins are bacterial and archaeal transcriptional regulators which mostly repress stress-responsive genes by binding to the promoter/operator region of the gene. For many MarR proteins, small ligand interactions or oxidation of cysteine residues attenuates this DNA-binding and initiates the stress response by allowing the gene to be expressed [3,4]. Of the two MarR homolog

Abbreviations: Asymmetric unit, AU; Hypothetical uricase regulator, HucR; Multiple antibiotic resistance regulator, MarR; Protein Data Bank, PDB.

* Corresponding author.

E-mail address: psy@ssu.ac.kr (S. Park).

proteins in the *D. radiodurans* genome [5,6], HucR (gene product of dr1159, Hypothetical uricase Regulator) binds tightly ($K_D=0.3~\rm nM$) to the intergenic region of *HucR* and the uricase gene (dr1160) [7]. Urate (metabolic breakdown product during the purine metabolism) which has been shown to have $K_D \sim 12~\mu M$ affinity to HucR antagonizes the HucR binding to the intergenic region [7,8]. The urate induced uricase (also known as the urate oxidase) expression may mainly function to decrease the urate concentration by oxidizating it to allantoin. However, because urate is a strong reducing agent (hence a well-known scavenger of reactive oxygen species), HucR has been suggested to take part in the oxidative stress response in *D. radiodurans* as well [7].

The previously reported crystal structure of HucR without the bound urate shows significant structural homology to other MarR structures of being a homodimer with triangular "saddle-like" topology [9]. The HucR structure further suggests that the aminoterminal α -helix (noted as α 1), which is absent in other MarR

homologs, contributes in forming a stable dimeric interface. Such a stable arrangement was believed to preconfigure the DNA recognition helices for DNA binding hence explaining the extraordinary sub-nanomolar affinity of HucR and the interacting DNA. Although urate has limited solubility in water, several protein structures have been reported in the presence of urate. For example, several rat (or bovine) xanthine oxidoreductase and fungal (or bacterial) uricase structures contain the urate either as the enzymatic product or substrate in the active site [10–13]. Furthermore, human glycogen phosphorylase has also been reported with the urate bound to the purine allosteric inhibitor site [14]. In this paper, we report the crystal structure of HucR determined with urate which has been soaked into the apo-HucR crystal. We analyze the urate interaction with HucR, and further compare the urate binding site to those of other urate binding proteins. We also suggest a mechanism, perhaps testable in the future, of how the urate may weaken the interaction between HucR and the cognate DNA.

2. Materials and methods

2.1. Protein expression and purification

The full-length gene encoding *D. radioduran* HucR (1~181) was inserted into pET28a vector for E. coli expression. The cloning was performed using NdeI and BamHI sites, and the final plasmid was sequence verified in the insert region. Chemically competent E. coli BL21(DE3) cells were transformed using the plasmid via heat shock, and the resulting cells grown on 1 L of LB broth containing 50 µg/ mL kanamycin at 37 °C. Over-expression of recombinant HucR was induced at $A_{600} = 0.6$ with 1 mM isopropyl- β -D-thiogalactopyranoside (IPTG). The cells were grown further at 27 °C overnight (16~20 h) and harvested using centrifugation at 11000×g. The harvested cell pellet was re-suspended in 5 mM imidazole, 25 mM Tris pH 7.5, and 500 mM NaCl buffer, and lysed using sonication in ice. The supernatant which contains the His6-tagged HucR protein was collected using centrifugation at 25000×g, and the contents poured over a column containing 5 mL of Ni-NTA agarose beads (Qiagen). The column was washed using four column volumes of 20 mM imidazole, 25 mM Tris pH 7.5, and 500 mM NaCl buffer, and the HucR protein eluted using 200 mM imidazole, 25 mM Tris pH 7.5, and 500 mM NaCl buffer. For His6-tag cleavage, the eluted HucR protein (~10 mL) was pooled and treated with bovine thrombin (MP Biomedicals, 0.25 U/ μ L as 20 \times) overnight at 4 °C. The HucR protein was loaded to HiLoad® 26/60 Superdex200® size-exclusion column (Cytiva) connected to AKTA FPLC (Cytiva), and was eluted using 50 mM Tris pH 7.5, and 150 mM NaCl buffer. The fractions under the chromatogram peak were concentrated using Amicon® Ultra centrifugal filter (Merck), and the protein concentration quantified by using the numbers of tyrosine and tryptophan in the HucR sequence (~5 mg/mL). The final HucR protein was flashfrozen in liquid nitrogen and was stored in -80 °C.

2.2. Crystallization and data collection

The apo-HucR crystals were obtained on a hanging drop setting at 4 °C using the previously reported condition (0.1 M Bis-Tris pH 7.0, 0.5 M MgCl₂ and PEG 3350 20-30%). Although urate is quite insoluble in water, several structures of proteins have been reported with urate either as a substrate or an allosteric regulator. Based on these previous studies, we soaked urate into the apo-HucR crystal by transferring a single crystal into a well-solution supplemented with final 10% (w/v) saturated water solution of uric acid sodium salt (Merck, U2875). Soaking was performed for 10 min, the crystal further dipped briefly into a cryo-protectant solution (well-solution with 45% (v/v) glycerol), and mounted on

a goniometer under a liquid nitrogen stream. X-ray diffraction data were collected on beamline 5C at Pohang Light Source (PLS, Pohang, Republic of Korea) using a CCD detector (Eiger 9 M). Data were auto-processed using AutoProcess in XDS [15] (SI Table 1).

2.3. Structure determination, refinement and analysis

The structure of apo-HucR (PDB code **2FBK**) [9] was used as the initial model to determine the urate soaked HucR structure. The location of urate was determined using the electron density map generated in COOT [16], and the entire structure further refined using REFMAC5 [17] (SI Table 1). The final HucR structure with urate was analyzed in COOT and PyMol (Schrödinger, LLC). All the structural figures were generated using PyMol.

3. Results and discussion

3.1. The overall structure of urate bound HucR

With the current experimental condition of urate soaking performed to the apo-HucR crystal, there seemed to be no structural changes either globally or locally compared to the apo-HucR structure. This was quite unexpected because the urate was observed in the structure (see below). In the urate bound HucR structure, the N-terminal (residues 1~7) and the C-terminal (residues 180~188) regions were not observed in the structure. As in the apo-HucR structure, the region connecting the $\alpha 1$ (the unique amino-terminal α -helix which is absent from other MarR homo- $\log s$) and $\alpha 2$ (HucR residues 26~34) was not observed also likely as a result of being disordered (Fig. 1). Also, as in the apo-HucR structure, the HucR residues of 121-128 which constitutes the loop connecting $\beta 2$ and $\beta 3$, the so-called wing motif which interacts with DNA, was not well-ordered. Although this region was not modeled in the apo-HucR structure (PDB code 2FBK) [9], we were able to see fair amount of electron densities at the F₀-F_c map contoured at 2σ , and have modeled them as much as we can in our deposited structure. However, the average thermal B-factor of 181 Å² in the region still inferred the innate flexibility. Even after the model building and refinement of this region, the electron density became completely connected at the 2Fo-Fc map only contoured at 0.6σ. When we analyzed the previous structure of apo-HucR with its deposited structure factors, the same electron densities were observed as well, suggesting that the observed density in this region was not the result of urate binding. As in the apo-HucR (PDB code 2FBK) [9], we have also observed a spherical electron density which was as strong as Cl⁻ and modeled it as such (Fig. 1). This Cl⁻ likely originates from the 0.5 M MgCl₂ in the crystallization condition. Interestingly, this Cl- was very close (3-4 Å) to the urate binding site (Fig. 1).

The lack of obvious structural changes with urate binding might be due to the inherent limit of the urate concentration achievable in our experimental setting and may not necessarily reflect the physiological concentration of urate in D. radiodurans. Although we have tried co-crystallizing HucR in the presence of urate, diffracting crystals did not appear in the crystallization condition saturated with urate. However, the absence of any notable change in the global or local (DNA interacting region especially of the WH motif) structures determined both with and without a ligand have been previously reported for other MarR proteins. For instance, E. coli MarR [18,19] and Sulfurisphaera tokodaii ST1710 MarR [20] do not show any structural differences upon salicylate binding, despite salicylate's known effect to attenuate DNA binding. However, DNA binding is found to induce significant changes in the WH motif in both cases. Also in Salmonella typhimurium SlyA, the WH motif is observed as disordered in both the presence and absence (apo-

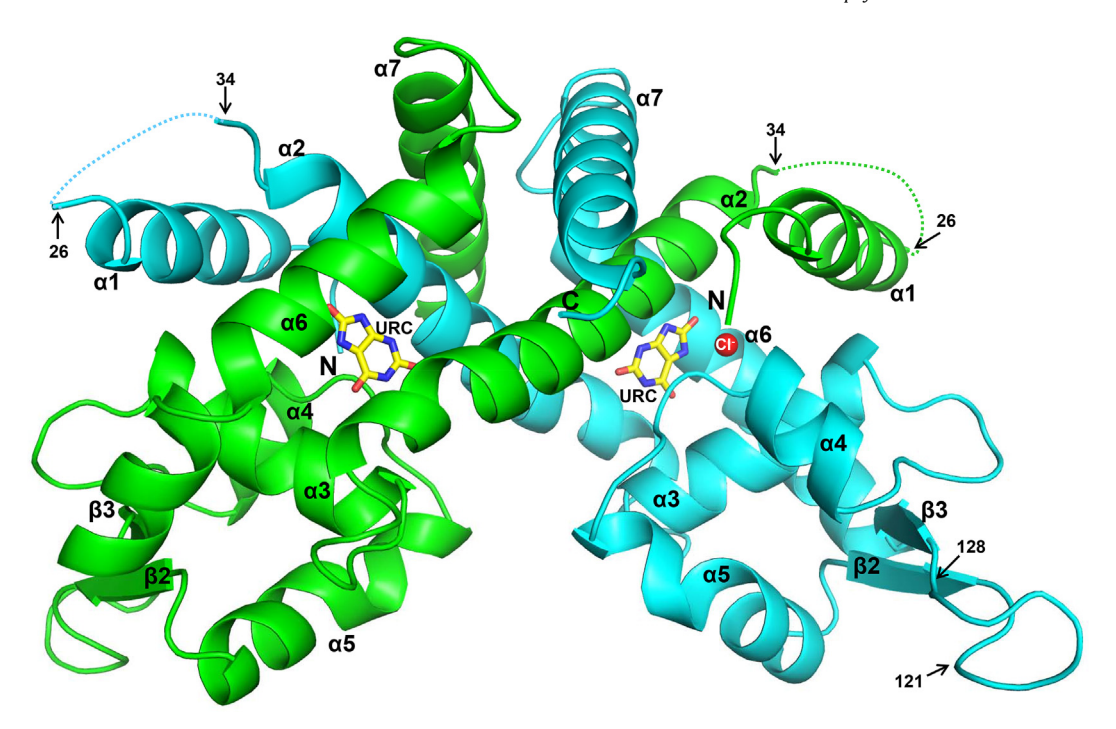


Fig. 1. The overall structure of HucR with the bound urate. The HucR structure (in ribbon) is shown with the bound urate (URC, in stick). Although there was only one molecule of HucR in the crystal AU, HucR is shown as the biologically relevant dimer (in different colors of cyan and green) with the interacting subunit generated using the crystallographic symmetry operation. HucR residues 26~34 are not observed in the electron density map, and the residues 121~128 (start and end residues indicated) have especially high B-factors reflecting conformational disorder in the region. Interestingly, a chloride ion (in sphere) is closely located near the urate (note that another Cl⁻ is hidden behind α6 and invisible in the figure.). (For interpretation of the references to color in this figure legend, the reader is referred to the Web version of this article.)

form) of bound salicylate, which only becomes ordered upon binding to the cognate DNA [21,22]. However, it is only fair to note that in other cases such as *Methanobacterium thermoautotrophicum* MTH313 MarR (from structures with and without salicylate) [23] and *Staphylococcus aureus* MarR (from structures with and without kanamycin) [24], respective binding of salicylate or kanamycin to the MarR protein induces changes in the MarR especially to the WH motif conformation (*see below for more discussions*).

3.2. The urate position in HucR

HucR crystallized with only one molecule in the crystal asymmetric unit as in the previous apo-structure. However, HucR formed a physiological dimer via the crystallographic symmetry mate as shown in Fig. 1. The electron density corresponding to the bound urate was located in the dimeric interface of the two dimeric subunits (Figs. 1 and 2). Although the presence of urate was evident in the F_0 - F_c OMIT map (contoured at 2.5 σ . Fig. 2A), the $2F_0$ - F_c map after urate modeling and refinement indicated both disorderness (the thermal B-factor of urate was 137.9 Å²) and low occupancy of the urate molecule (Fig. 2B). When the urate location was compared against the previous HucR structure (PDB code 2FBK), well-ordered water molecules were found to occupy the site (Fig. 2 C&D). Several structures of MarR have been reported with a ligand bound to the corresponding urate site of HucR (Fig. 3). For example, salicylates at the similar location are found to be interacting with MarR of S. tokodaii ST1710 (Fig. 3A), S. typhimurium SlyA (Fig. 3B) and M. thermoautotrophicum MTH313 (Fig. 3C). Of note, between the different salicylate locations reported M. thermoautotrophicum MTH313 (noted as "SAL1" and "SAL2" in ref.23), the location of urate in HucR corresponded to "SAL1" which is 3 Å away from the urate in the superposed structures. ("SAL2" is ~7 Å away from the urate). Kanamycin is also observed to be bound at the similar location in the case of S. aureus MarR (Fig. 3D).

Such disorder in the urate might result from the low affinity of urate to HucR, which is of $K_D \sim \! 12~\mu M$ [8]. In fact, in other examples of urate bound either as an enzymatic product (or substrate) in the active site or as an allosteric inhibitor in other proteins much higher ordering is observed (see below) likely from the strong urate interaction with the protein. Hence, the disorderness of the bound urate might be natural given the fact that HucR is a MarR family protein and may therefore be designed to bind to a broad family of compounds rather than being limited to urate binding. Together with the low affinity of urate, the low solubility of the urate itself might be another plausible explanation because the average thermal B-factors of salicylate and kanamycin are all $40{\sim}60~\textrm{Å}^2$ in the structures of Fig. 3.

3.3. The detailed interaction of urate with HucR

The urate observed in the HucR was located in a hydrophobic pocket formed by Trp20 (α 1) and Met41/Leu44/Leu45 (all from α 2) of one subunit, and Ile58 (α 2)/Trp72 (α 3) and Ala97/Ile98 (both of the α 4- α 5 loop) of the other subunit (Fig. 4A). Other than the hydrophobic interactions from the surrounding residues, the urate binding was further mediated by possible hydrogen bonding interactions of Met41/Leu44/Leu45 (via main-chain), Trp20 (α 1)/Glu48 (α 2) (via side-chain) of one subunit, and of Ala69 (from α 3) (via main-chain), Asp73 (from α 3)/His147 (from α 6) (via side-chain) of the other subunit (Fig. 4B). Also, multiple water molecules were involved in the formation of a network for the binding (Fig. 4B). Despite the fact that the urate binding pocket appears to be a conserved ligand binding location for some MarR proteins, the residues whose side chains are involved in the urate interaction are not conserved among other MarR proteins.

In PDB, mammalian (rat and bovine) xanthine oxidoreductase [10] and fungal (or bacterial) uricase structures are reported with urate either as the enzymatic product or substrate in the active site [11–13]. Also, the structure of human glycogen phosphorylase has

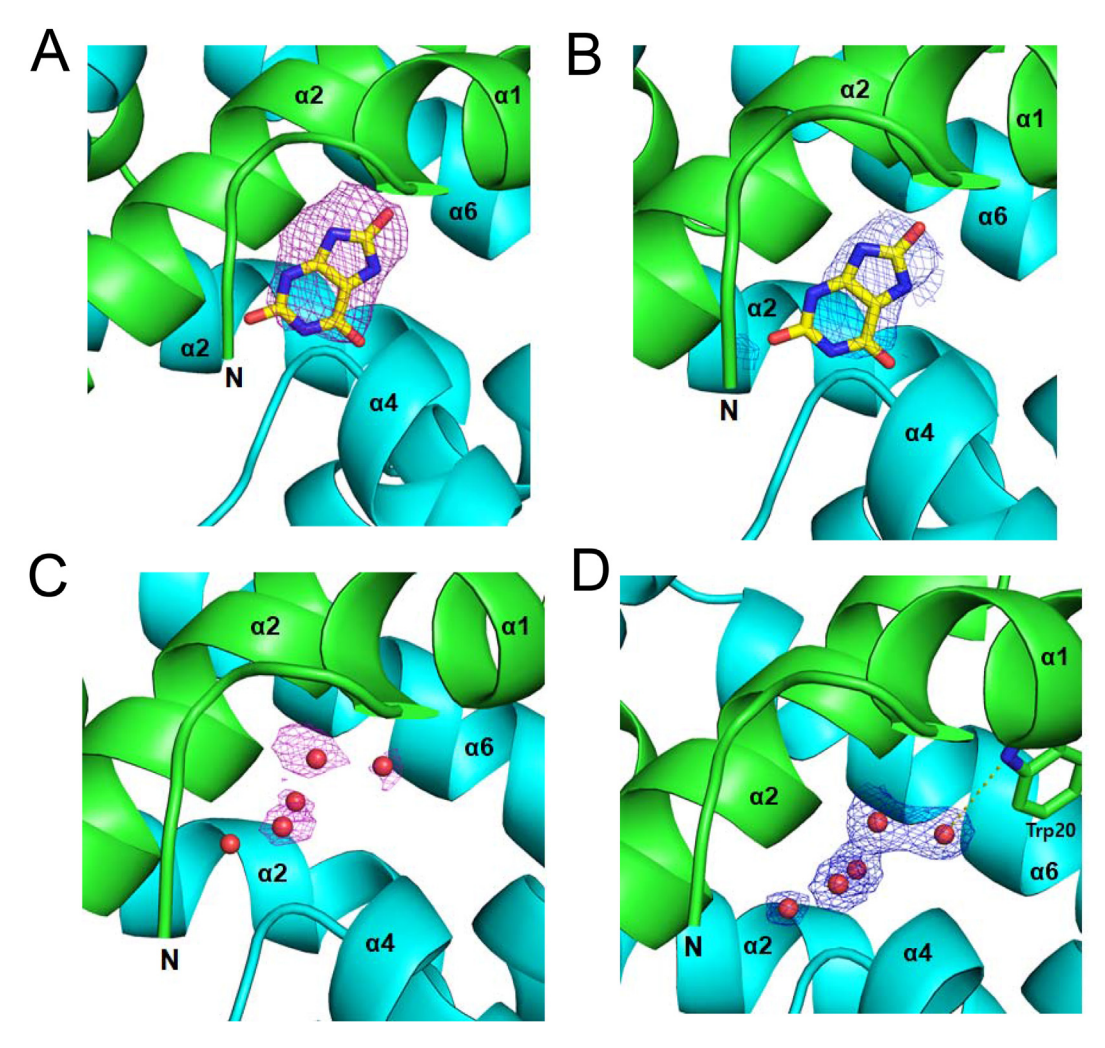


Fig. 2. The electron densities of urate (A and B) and waters (C and D), respectively, for the urate soaked HucR crystal and the apo-HucR crystal structures. The OMIT electron density (F_o-F_c) map contoured at (2.5σ) indicates a bound urate molecule at the site (A). The broad electron density over urate $(2F_o-F_c)$ map contoured at (2.5σ) suggests that the urate is disordered and partially occupied at the site (B). In the previous HucR structure (PDB code **2FBK**), the urate binding site is occupied by several water molecules as shown in the electron density maps (C, water OMIT F_o-F_c map contoured at (2.5σ) ; D, $(2F_o-F_c)$ map contoured at (2.5σ)

been determined with the urate bound to the purine allosteric inhibitor site [14]. In these cases, urates are found to be more ordered than our case. The molecular interactions stabilizing the bound urate are also different compared to those in Huck. For instance, direct hydrogen bonding (or electrostatic) interactions of arginine and glutamate to urate are notable in the cases of xanthine oxidoreductase [10], Aspergillus flavus uricase [11] and Arthrobacter globiformis uricase [12]. In the flavin-dependent Klebsiella pneumonia uricase [13], arginine, aspartate and also a water molecule linked by these two residues are important in mediating the urate interaction. For the human glycogen phosphorylase, glutamate, aspartate, asparagine residues and a water network (via multiple water molecules) are responsible for stabilizing the urate [14]. Hence, the urate interaction in HucR with histidine (His147) and glutamate (Glu48) residues directly contacting the urate along with ordered waters which are stabilized by various residues (Glu48, Trp20, Asp73) is quite unique compared to other known cases of urate and protein interaction.

3.4. How can the urate mediate inhibition of HucR and the cognate DNA interaction?

Our HucR structure in the presence of urate when compared to the apo-form indicated that no significant conformational change occurs with the urate binding. Intuitively, since apo-HucR acts as a repressor binding to the cognate DNA, its ligand, urate, should be expected to change the HucR structure compared to the apo-form to limit the physiological binding of the DNA. Such change in the local structure of MarR is found in the M. thermoautotrophicum MTH313 MarR where salicylate binding changes the MarR structure near the WH motif from a "closed" form (apt for DNA binding) to an "open" form (unable to bind DNA) [23]. Similar changes are observed for the S. aureus MarR upon kanamycin binding [24]. However, there are other reports where ligand binding by itself does not alter the MarR structure. For instance, in E. coli MarR, both the apo-form and the salicylate-bound form are nearly identical, although the DNA-bound form undergoes a significant change to accommodate proper interaction with the DNA [18,19,25]. From these structural comparisons of the apo- and the salicylate-bound forms to the DNA-bound MarR, the authors conclude that the non-DNA bound (apo- and salicylate-bound) MarR adopted a conformation incapable of DNA-binding [19]. Also, in the S. tokodaii ST1710 MarR, no significant changes in structure are observed between the apo-form and the salicylate-bound form. Intriguingly, the DNA-bound form of the S. tokodaii ST1710 MarR also indicates a similar local structure as the non-DNA bound form, suggesting that both the apo-form and the salicylate-bound form are already in a pre-configured state necessary for DNA binding [20]. In addition,

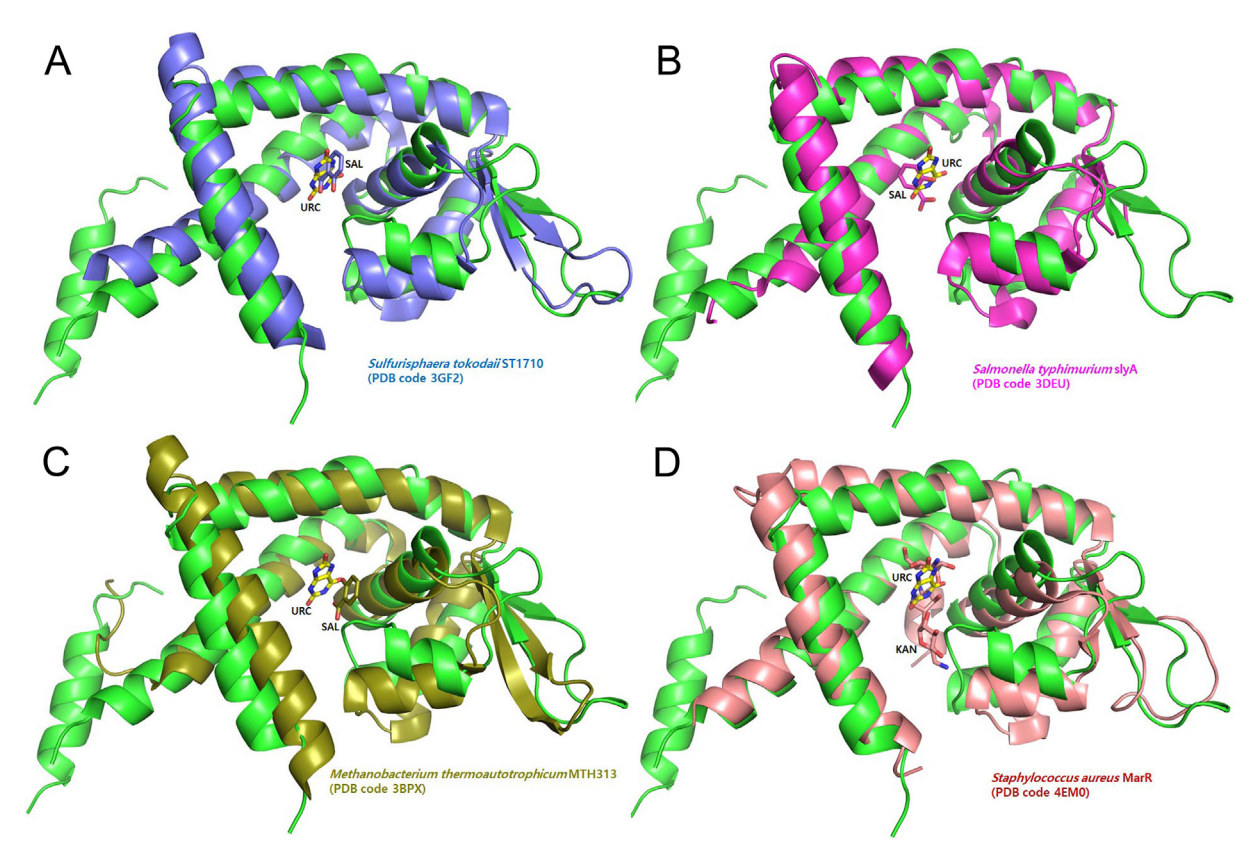


Fig. 3. The urate binding site in HucR corresponds to the salicylate (A–C) and kanamycin (D) interaction sites in other MarR proteins. When superimposed to the structures of several other MarRs with bound ligands, the corresponding urate binding site in HucR holds other ligand molecules such as salicylate (A–C) and kanamycin (D). Of note, the salicylate shown in the *M. thermoautotrophicum* MTH313 MarR structure (C) corresponds to the "SAL1" location in the ref. 23.

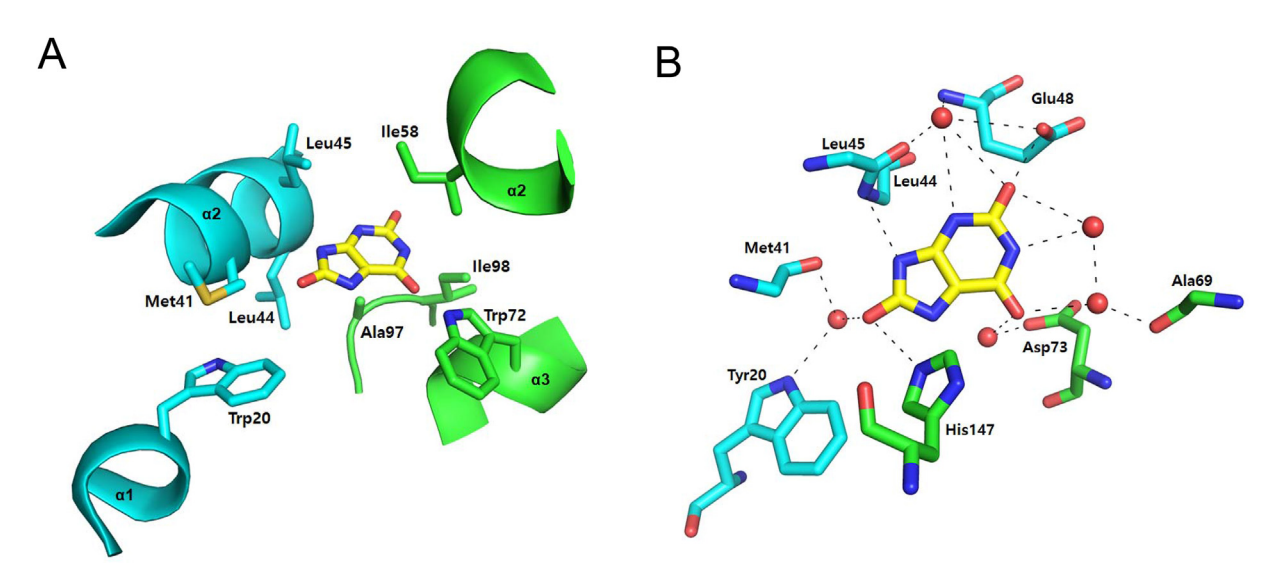


Fig. 4. The detailed urate binding interactions in HucR. The urate observed in the hydrophobic pocket of HucR is shown (A). The HucR residues and waters mediating polar urate interaction are shown (B). The interacting atoms were selected using distance criteria typically allowed for a hydrogen bonding. The urate is located at the dimer interface of the two HucR subunits indicated with different colorings (cyan and green). (For interpretation of the references to color in this figure legend, the reader is referred to the Web version of this article.)

the *S. typhimurium* SlyA structures both in the absence (apo-form) and in the presence of salicylate were mostly identical with the WH motif disordered. However, in the DNA-bound form, the WH motif becomes more ordered without other significant changes happening in the structure [21,22]. Taken together, both the apoform and the salicylate-bound form of *S. typhimurium* SlyA and

the *S. tokodaii* ST1710 MarR can be regarded to be in the preconfigured state for DNA binding (unlike in the cases for the *M. thermoautotrophicum* MTH313 and *S. aureus* MarRs).

Given these observations of various MarR structures without a ligand and with a ligand (or with DNA-bound), it is difficult to conclude at this moment whether our identically structured HucR

both in the absence and in the presence of the urate represents a MarR form configured to bind its cognate DNA or a form which may undergo changes upon DNA binding. As noted above, the identically structured apo- and salicylate-bound MarRs in some cases (*S. tokodaii* ST1710 MarR and *S. typhimurium* SlyA) are already preconfigured to the DNA-bound form resulting in no significant conformational change upon DNA binding, whereas in the case of *E. coli* MarR, both states are unable to bind to DNA, with the conformational change suitable for binding occurring upon the interaction with the cognate DNA. In other words, it cannot be concluded whether or not the previously reported apo-form of HucR can bind to its cognate DNA without changes in the conformation. Hence, a future DNA-bound HucR structure would be helpful in further envisioning how urate impedes binding of HucR to its cognate DNA binding.

Based on our structure, another inference to this question on urate mediated interference of DNA-binding can be made from the observation that Trp20 of α 1 helix actively participates in the urate binding both via hydrogen bonding and van der Waals interaction (Fig. 4). In the apo-form of HucR, the site of urate binding is occupied by multiple water molecules forming a hydrogen bonding network, that is connected to the side chain of Trp20 as well (Fig. 2D). The strong sub-nanomolar DNA interaction of HucR was proposed to result from the $\alpha 1$ helix which stabilizes the dimerization interface and preconfigures the DNA recognition helices for proper cognate DNA binding, and the tight associations of waters observed at the urate site may also be important in mediating this stability. Hence, there is a possibility that the reorganization of these water molecules upon urate binding has the effect of altering the stability of the preconfigured dimer (perhaps in solution and not necessarily in the crystal state) to attenuate HucR's interaction with DNA. Although the three-fold lowered binding affinity of Huck-W20F mutant to the cognate DNA compared to the wild-type HucR [26] may partly support this idea, further experiments are necessary to test this hypothesis.

3.4.1. PDB accession code

Coordinates and structure factors of HucR with urate have been deposited in the RCSB PDB with accession code **7XL9**.

Funding

This research was supported by Basic Science Research Program through the National Research Foundation of Korea (NRF) funded by the Ministry of Education (2021R1A6A1A10044154). Experiment at Pohang Light Source (PLS) was supported in part by MEST and Pohang University of Science and Technology.

Authors contribution

S.P. and S.P.W. devised the experiment. S.P.W. cloned the HucR construct. J.K.P. produced the protein and the crystal. T.P. and B.I.L performed the diffraction experiment and reduced the data. S.P., W.J., S.R., M.H.C., M.K., J.K. and J.B. determined and analyzed the structure. All the authors co-wrote the manuscript.

Declaration of competing interest

The authors declare no conflict of interest.

Acknowledgements

The authors would like to thank the staff at PAL 5C for their support and beam time.

Appendix A. Supplementary data

Supplementary data to this article can be found online at https://doi.org/10.1016/j.bbrc.2022.05.034.

References

- D.M. Sweet, B.E.B. Moseley, The resistances of Micrococcus radiodurans to killing and mutation by agents which damage DNA, Mutat. Res. 34 (1976) 175–186, https://doi.org/10.1016/0027-5107(76)90122-6.
- [2] J.R. Battista, A.M. Earl, M.J. Park, Why is Deinococcus radiodurans so resistant to ionizing radiation? Trends Microbiol. 7 (1999) 362–365, https://doi.org/ 10.1016/S0966-842X(99)01566-8.
- [3] A. Grove, MarR family transcription factors, Curr. Biol. 23 (2013) R142—R143, https://doi.org/10.1016/j.cub.2013.01.013.
- [4] D.K. Deochand, A. Grove, MarR family transcription factors: dynamic variations on a common scaffold, Crit. Rev. Biochem. Mol. Biol. 52 (2017) 595–613, https://doi.org/10.1080/10409238.2017.1344612.
- [5] K.S. Makarova, L. Aravind, Y.I. Wolf, et al., Genome of the extremely radiation-resistant bacterium Deinococcus radiodurans viewed from the perspective of comparative genomics, Microbiol. Mol. Biol. Rev. 65 (2001) 44–79, https://doi.org/10.1128/MMBR.65.1.44-79.2001.
- [6] O. White, J.A. Eisen, J.F. Heidelberg, et al., Genome sequence of the radioresistant bacterium Deinococcus radiodurans R1, Science 286 (1999) 1571–1577, https://doi.org/10.1126/science.286.5444.1571.
- [7] S.P. Wilkinson, A. Grove, HucR, a novel uric acid-responsive member of the MarR family of transcriptional regulators from Deinococcus radiodurans, J. Biol. Chem. 279 (2004) 51442-51450, https://doi.org/10.1074/ ibc M405586200
- [8] S.P. Wilkinson, A. Grove, Negative cooperativity of uric acid binding to the transcriptional regulator HucR from Deinococcus radiodurans, J. Mol. Biol. 350 (2005) 617–630, https://doi.org/10.1016/j.jmb.2005.05.027.
- [9] T. Bordelon, S.P. Wilkinson, A. Grove, et al., The crystal structure of the transcriptional regulator HucR from Deinococcus radiodurans reveals a repressor preconfigured for DNA binding, J. Mol. Biol. 360 (2006) 168–177, https://doi.org/10.1016/j.jmb.2006.05.005.
- [10] T. Nishino, K. Okamoto, Y. Kawaguchi, et al., The C-terminal peptide plays a role in the formation of an intermediate form during the transition between xanthine dehydrogenase and xanthine oxidase, FEBS J. 282 (2015) 3075–3090, https://doi.org/10.1111/febs.13277.
- [11] L. Gabison, M. Chiadmi, M. El Hajji, et al., Near-atomic resolution structures of urate oxidase complexed with its substrate and analogues: the protonation state of the ligand, Acta Crystallogr. D66 (2010) 714–724, https://doi.org/ 10.1107/S090744491001142X.
- [12] E.C.M. Juan, M.M. Hoque, S. Shimizu, et al., Structures of Arthrobacter globiformis urate oxidase-ligand complexes, Acta Crystallogr. D64 (2008) 815–822, https://doi.org/10.1107/S0907444908013590.
- [13] K.A. Hicks, S.E. O'Leary, T.P. Begley, et al., Structural and mechanistic studies of HpxO, a novel flavin adenine dinucleotide-dependent urate oxidase from Klebsiella pneumoniae, Biochemistry 52 (2013) 477–487, https://doi.org/ 10.1021/bi301262n
- [14] J.L. Ekstrom, T.A. Pauly, M.D. Carty, et al., Structure-activity analysis of the purine binding site of human liver glycogen phosphorylase, Chem. Biol. 9 (2002) 915–924, https://doi.org/10.1016/S1074-5521(02)00186-2.
- [15] W. Kabsch, XDS, Acta Crystallogr. D66 (2010) 125–132, https://doi.org/
- [16] P. Emsley, K. Cowtan, Coot: model-building tools for molecular graphics, Acta Crystallogr. D60 (2004) 2126–2132, https://doi.org/10.1107/ S0907444904019158.
- [17] G.N. Murshudov, P. Skubák, A.A. Lebedev, et al., REFMAC5 for the refinement of macromolecular crystal structures, Acta Crystallogr. D67 (2011) 355–367, https://doi.org/10.1107/S0907444911001314.
- [18] M.N. Alekshun, S.B. Levy, T.R. Mealy, et al., The crystal structure of MarR, a regulator of multiple antibiotic resistance, at 2.3 Å resolution, Nat. Struct. Mol. Biol. 8 (2001) 710–714, https://doi.org/10.1038/90429.
- [19] R. Zhu, Z. Hao, H. Lou, et al., Structural and mechanistic study of the cysteine oxidation-mediated induction of the Escherichia coli MarR regulator, Tetrahedron 73 (2017) 3714–3719, https://doi.org/10.1016/j.tet.2017.05.039.
- [20] T. Kumarevel, T. Tanaka, T. Umehara, et al., ST1710-DNA complex crystal structure reveals the DNA binding mechanism of the Mark family of regulators, Nucleic Acids Res. 37 (2009) 4723–4735, https://doi.org/10.1093/nar/ gkn496
- [21] W.R. Will, P. Brzovic, I. Le Trong, et al., The evolution of SlyA/RovA transcription factors from repressors to countersilencers in enterobacteriaceae, mBio 10 (2019) e00009–19, https://doi.org/10.1128/mBio.00009-19.
- [22] K.T. Dolan, E.M. Duguid, C. He, Crystal structures of SlyA protein, a master virulence regulator of Salmonella, in free and DNA-bound states, J. Biol. Chem. 286 (2011) 22178–22185, https://doi.org/10.1074/jbc.M111.245258.
- [23] V. Saridakis, D. Shahinas, X. Xu, et al., Structural insight on the mechanism of regulation of the MarR family of proteins: high-resolution crystal structure of a transcriptional repressor from Methanobacterium thermoautotrophicum, J. Mol. Biol. 377 (2008) 655–667, https://doi.org/10.1016/j.jmb.2008.01.001.

- [24] Y.M. Chang, C.K.M. Chen, T.P. Ko, et al., Structural analysis of the antibiotic-recognition mechanism of MarR proteins, Acta Crystallogr. D69 (2013) 1138–1149, https://doi.org/10.1107/S0907444913007117.
- [25] R. Zhu, Z. Hao, H. Lou, et al., Structural characterization of the DNA-binding mechanism underlying the copper(II)-sensing MarR transcriptional regulator, J. Biol. Inorg. Chem. 22 (2017) 685–693, https://doi.org/10.1007/
- s00775-017-1442-7.
- [26] I.C. Perera, Y.H. Lee, S.P. Wilkinson, et al., Mechanism for attenuation of DNA binding by MarR family transcriptional regulators by small molecule ligands, J. Mol. Biol. 390 (2009) 1019–1029, https://doi.org/10.1016/j.jmb.2009.06.002.